

# Stability analysis of aircraft's sudden damage process with ROA overlapping

Jie Chen, Cunbao Ma and Dong Song

School of Aeronautics, Northwestern Polytechnical University, Xi'an, China

## Abstract

**Purpose** – The paper aims to propose a stability analysis method based on region-of-attraction (ROA) overlapping to evaluate the flight stability of the possible sudden damage process and guarantee flight safety in extreme cases.

**Design/methodology/approach** – First, according to the two flight conditions before and after damage which the aircraft may encounter, flight dynamical models are built and fitted by polynomial equation for subsequent ROA analysis. And then, the ROA overlapping estimation method based on V-s iteration is presented to complete the stability analysis of such airplane sudden damage process.

**Findings** – Finally, in the presence of control surface damage, case aircraft flight stability is analyzed and simulated to verify the effectiveness of the proposed method.

**Practical implications** – The proposed method can be used for stability check during the aircraft control law design, or for further completing the design of the emergency stable controller design.

**Originality/value** – Compared with previous studies on sudden damage process of aircraft, to the best of the authors' knowledge, this is one of the pioneer studies in which the ROA and ROA overlapping concept has been introduced. This study on stability analysis of aircraft sudden damage process could further develop the theory of emergency stable control.

**Keywords** Stability analysis, Flight safety, Region-of-attraction, Sudden damage

**Paper type** Research paper

## Introduction

In recent years, the frequent occurrence of flight accidents presents severe challenges to aviation safety, and it is urgent to improve the aircraft's stability or safety in extreme conditions. Although the stability of aircraft has been greatly improved by the introduction of modern advanced control technology under normal conditions, the flight safety is a great threat by the damage in some extreme conditions and sudden accidents, which may result in a significant loss of lives and properties. Thus, the aircraft's stability in extreme conditions has attracted increasing attentions by many scholars and institutes; the NASA's Aviation Safety Program planned to reduce the fatal aircraft accident rate by 80 per cent by 2007, and by 90 per cent by 2022 (Belcastro, 2003). Affected by the unexpected events (such as system failure, fire attack and bird hit damage), aircraft's system parameters will suddenly change. This variation will deteriorate aircraft's handling characteristics, break the original aerodynamic balance and moreover, lead to crash. However, the traditional system design procedure does not consider the sudden instability problem.

In theory, the effect caused by aircraft's sudden damage can be seen as the controlled model parameters' unplanned variation. Specifically, the flight state is continuous at sudden

instability moment, whereas the model parameters and system stability region are not, that is to say, the two system stability regions before and after damage are different. So if these two regions have overlapping part and meanwhile the flight state point at the mutation moment is included in this overlapping part, then the aircraft's stability and flight safety can be guaranteed.

Aircraft model's mutation and the resulting instability are differences in the "mutations" in nonlinear mathematic field (smooth system's state discontinuous variation, cusp or manifold folding, while the continuous variation of external conditions or system parameters). In the former situation, the state is continuous and the parameter is mutational, whereas the latter one is of mutational state and continuous parameter. As the damage is unknown, sudden and arbitrary, the stability analysis of aircraft is difficult. At present, some exploratory research has been carried out. Shorten *et al.* (2003) presented the necessary and sufficient conditions for the existence of a common quadratic Lyapunov function for a pair of dynamic systems whose system matrices  $A_1$  and  $A_2$

*Conflict of interest and funding statement:* There are no conflicts of interest.

The authors would like to thank the Editors and the anonymous reviewers for critical and constructive comments that helped to improve the quality and presentation of this paper. They would also like to thank Yang CW and Wen YL for valuable discussions on the dynamical modeling. This work was supported by the National Key Basic Research Program of China (Grant No. 2014CB744900), the Fundamental Research Funds for the Central Universities (Grant No.3102018ZY003) and Aeronautical Science Foundation of China (Grant No. 2016553035).

Received 13 August 2016

Revised 18 December 2016

Accepted 2 January 2017

The current issue and full text archive of this journal is available on Emerald Insight at: [www.emeraldinsight.com/1748-8842.htm](http://www.emeraldinsight.com/1748-8842.htm)



Aircraft Engineering and Aerospace Technology  
90/2 (2018) 398–411  
© Emerald Publishing Limited [ISSN 1748-8842]  
[DOI 10.1108/AEAT-08-2016-0127]

are in companion form. Cheng (2004) showed this process's stability problem by Lie algebra and Lie group, and provided the necessary and sufficient condition for the system to be quadratically stabilized. System's region-of-attraction (ROA) analysis and estimation are a complex and meaningful problem. In the early 1990s, Jackson and Kodoeorgiou (1992) analyzed and pointed out that, even in a simple two-dimensional low-order system, ROA may be very complex, or even have bifurcation. There are two research methods for ROA estimation, namely, analytical analysis and numerical calculation: analytical one can be used to accurately solve the system's ROA (Jia et al., 2005; Yang, 2012; Tu et al., 2012), as the ROA boundary is generally composed by the stable and unstable manifold of equilibrium point; such method is also called as manifold estimation method (Chen, 2009). However, analytical method is often unfeasible for complex systems, whereas several numerical calculation methods can solve such problems very well, in which the continuous algorithm has been widely concerned. Rezgui and Lowenberg (2014) analyzed the global stability region of helicopter in hover and forward with the propeller blade leading slat by continuous algorithm.

The commonly used method for ROA estimation in control field is the numerical solution based on the Lyapunov function. This method constructs the Lyapunov convex function at equilibrium point, and then constraints or guarantees that the state's trajectory is convergent to stable fixed point by the function's negative definite. Moreover, the optimal convex boundary (i.e. ROA boundary) is obtained. As the solution of the Lyapunov convex function is concerned with the system's semi-definite programming (SDP) problem, which is described by the polynomial, Parrilo (2000) developed SOSTOOLS. This software tool decomposes polynomial by sum of squares (SOS), constructs the convex quadratic inequalities and completes the convex optimal problem of the Lyapunov function (Prajna, 2005; Papachristodoulou, 2005; Tan, 2006). After that, the ROA analysis based on SOS became a hot spot (Amato et al., 2011; Chesi, 2011). In this paper, based on the nonlinear dynamic system's ROA estimation theory (i.e. local asymptotically stable region), the stability analysis of the aircraft's sudden damage process is completed by the ROA overlapping analysis.

### Sudden damage' effect on aircraft model

In this paper, the physical damage of control surface is taken as a case to investigate the sudden damage effect. Control surface's damage affects both the control efficiency and aircraft's aerodynamic characteristic.

The general aircraft's linear longitudinal equation is assumed to be (Brian and Frank, 1992):

$$\begin{aligned} \dot{V} &= [G_{xa} + (T + F_x)\cos\alpha + F_z\sin\alpha]/m \\ \dot{\alpha} &= \frac{1}{mV} [G_{za} + F_z\cos\alpha - (T + F_x)\sin\alpha] + q \\ \dot{q} &= M/\mathcal{J}_y \\ \dot{\theta} &= q \end{aligned} \tag{1}$$

where  $\dot{V}$  is the airspeed of aircraft,  $\alpha$  is the angle of attack,  $\theta$  is the pitch angle of aircraft,  $\dot{q}$  is the pitch angle rate,  $T$  is the engine's thrust,  $F_x$  and  $F_z$  are total force components along  $x$ -axis and  $z$ -axis in aircraft's body frame,  $F_x = QSC_{x_{tot}}$  and  $F_z = QSC_{z_{tot}}$  in which  $Q$  is the dynamic pressure and  $C_{x_{tot}}$  and  $C_{z_{tot}}$  are total force coefficients in different axes in aircraft's body frame,  $m$  is the mass of aircraft,  $\begin{bmatrix} G_{xa} \\ G_{za} \end{bmatrix} = \begin{bmatrix} mg\sin(\alpha - \theta) \\ mg\cos(\alpha - \theta) \end{bmatrix}$ ,  $G_{xa}$  and  $G_{za}$  are the aircraft's weight component in  $x$ - and  $z$ -axes in airflow frame,  $g$  is gravitational acceleration,  $M = QSc_A C_{m_{tot}}$ ,  $C_{m_{tot}}$  is the total moment coefficient in aircraft's body frame and  $\mathcal{J}_y$  is the aircraft's moment of inertia around the  $y$ -axis in body frame.

Take the aircraft's total moving tail damage as example to explain: When the tail is damaged seriously, the corresponding total aerodynamic force and moment coefficient to tail in vertical axis will decrease, i.e.  $C_{xt} \rightarrow C'_{xt}$ ,  $C_{mt} \rightarrow C'_{mt}$ , which will lead to the variation of lift and pitch moment coefficients to  $\alpha$ , i.e.  $C_{x\alpha} \rightarrow C'_{x\alpha}$ ,  $C_{m\alpha} \rightarrow C'_{m\alpha}$ . These two parameters are the main items in lift and pitch moment equations, whose variation will affect the aircraft longitudinal force and moment, and then make aircraft body motion characteristic variation. Meanwhile, control surface's structure damage will change the aircraft mass and mass distribution, and then affect the momentum moment and center of gravity (c.g.) of aircraft.

To complete the stability analysis based on the ROA overlapping, the damage effects on aerodynamic force and moment coefficient are simplified as a proportional factor multiplied on these:

$$C'_{i\delta_j} = k_{\delta_j} C_{i\delta_j} \tag{2}$$

where the subscript  $i$  is the force and moment symbol which can be defined as lift  $F_z$ , drag  $F_x$ , side force  $F_y$ , roll moment  $L$ , pitch moment  $M$  and yaw moment  $N$ ;  $\delta_j$  is the control surface, such as elevator  $\delta_e$ , rudder  $\delta_r$ , aileron  $\delta_a$ ; and  $k_{\delta_j}$  is the damage proportional factor for different control surfaces.

In longitudinal plane, the total moving tail's damage mainly affects the lift and pitch moment coefficient, and the effect on drag coefficient can be neglected. To describe the aircraft models with sudden damage, the total lift and pitch moment coefficient which is relative to elevator  $C_{i\delta_e}$  can be replaced by  $C'_{i\delta_e}$ , i.e:

$$C'_{z_{tot}} = C'_{z}(\alpha, \beta, \delta_e) + \frac{c}{2V} \cdot C_{zq}(\alpha) \cdot q \tag{3}$$

$$C'_{m_{tot}} = C'_{m}(\alpha, \delta_e) + C'_{z_{tot}} \cdot (x_{cgr} - x_{cg}) + \frac{c}{2V} \cdot C'_{mq}(\alpha) \cdot q \tag{4}$$

And then equations (3) and (4) can be substituted back into the equation (1) mentioned above to get the aircraft models after the control surface's damage.

According to the different damage degree of total moving tail, the damage proportional factor  $k_{\delta_j}$  is different. In this paper, we choose three damage coefficients to build the damage models and verify the proposed method, which are  $k_{\delta_e} = 0.7$

(damage 30 per cent),  $k_{\delta_e} = 0.5$  (damage 50 per cent) and  $k_{\delta_e} = 0.2$  (damage 80 per cent).

### Aircraft polynomial fitting model

In this paper, the aerodynamic data of F-16 in NASA have been chosen as the research case (Russell, 2003), and have been used to build the aircraft’s model before and after damage; the configuration data are shown as Table I.

As the system’s ROA analysis based on the Lyapunov function is established by the polynomial semi-definite programming (SDP), a large number of non-polynomial items (such as: angle cosine matrix, engine thrust nonlinearity and aerodynamic parameters) in the traditional aircraft’s differential equation (1) need to be fitted by polynomial, in which:

The  $\cos(\alpha - \theta)$  and  $\sin(\alpha - \theta)$  are expanded by Taylor series and truncated at the first two items:

$$\sin(\alpha - \theta) \approx (\alpha - \theta) - \frac{1}{6}(\alpha - \theta)^3,$$

$$\cos(\alpha - \theta) \approx 1 - \frac{1}{2}(\alpha - \theta)^2,$$

where  $|(\alpha - \theta)| \leq \frac{\pi}{4}$ .

The  $\frac{1}{V}$  can be fitted by multivariate nonlinear polynomial as:

$$\frac{1}{V} \approx 5.7482 \times 10^{-3} - 1.0357 \times 10^{-5} \times V + 5.8897 \times 10^{-9} \times V^2 \quad V \subseteq [300ft/s \quad 900ft/s],$$

And the fitting effect of  $\frac{1}{V}$  is shown in Figure 1 below.

The  $C_{z}(\alpha, \beta, \delta_e)$ ,  $C_{zq}(\alpha)$ ,  $C_m(\alpha, \delta_e)$ ,  $C_{mq}(\alpha)$  and their damage items in equations (3) and (4) can be calculated by the aerodynamic data (Russell, 2003) and by equation (2). And then, on the basis of the multivariate nonlinear polynomial method, all the aerodynamic coefficient expression can be fitted, in which the order of fitted polynomials is not more than three times. For the fitting process, the angle ranges of aerodynamic data are restricted as given in Table II, and the partial data fitting effect can be shown in Figures 2 to 5.

By substituting all these parameters’ polynomial expression into F-16’s longitudinal equation (1), the longitudinal four-state

Table I Aircraft and environment parameter

Gravity (g)	32.17 ft/s <sup>2</sup>
Mass (m)	636.94 slugs
Span (B)	30.0 ft
Wing area (S)	300 ft <sup>2</sup>
Geometric mean chord length ( $\bar{c}$ )	11.32 ft
c.g. ( $\bar{x}_{cg}$ )	0.30
$J_y$	55,814.0 slug-ft <sup>2</sup>
$J_{xz}$	982.0 slug-ft <sup>2</sup>
Reference c.g. position( $\bar{x}_{cgr}$ )	0.35
$J_z$	63,100.0 slug-ft <sup>2</sup>
$J_x$	9,496.0 slug-ft <sup>2</sup>
Air density ( $\rho$ )	1.224 kg/m <sup>3</sup>

Figure 1 The fitting effect of 1/V

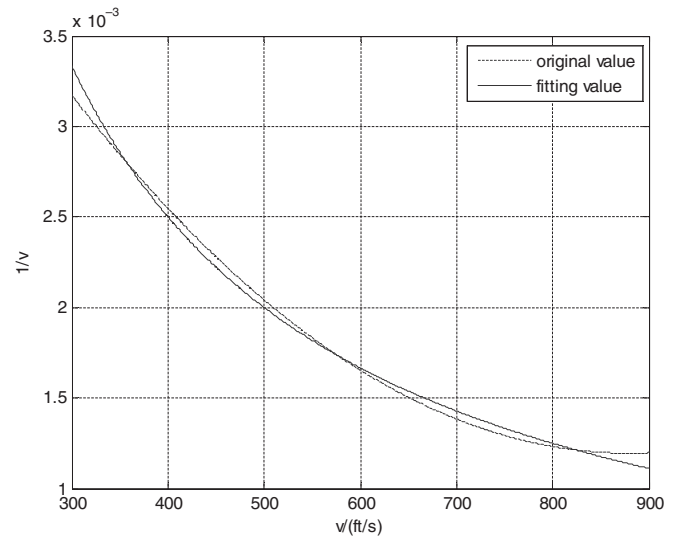


Table II Fitting angle range

Flight state parameter	Fitting range		Raw data range (deg)
	(deg)	(rad)	
$\alpha$	(-5 to 15)	(-0.09 to 0.26)	(-10 to 45)
$\delta_e$	(-25 to 25)	(-0.43 to 0.43)	(-25 to 25)
$\beta$	(-10 to 10)	(-0.17 to 0.17)	(-)

polynomial normal and un-normal model can be determined; these four states are  $[V, \alpha, q \text{ and } \theta]$  and the two inputs are  $[T \text{ and } \delta_e]$ , and this specific model is shown in the Appendix.

### The region-of-attraction overlapping estimation method based on V-s iteration

To complete the stability analysis of aircraft’s sudden damage process, the polynomial equation (i.e. aircraft model) stability region should be analyzed. In this section, the ROA estimation method was introduced to complete the stability analysis.

#### Region-of-attraction estimation

The ROA of system, in other word, the local asymptotic stability region of the system, is defined as: for the nonlinear polynomial autonomous system:

$$\dot{x} = f(x), x \in R^n, x(0) = x^0 \quad (5)$$

where  $f(x)$  is the polynomial function with variation  $x$ , and  $f(0) = 0$ , the original state point is assumed to be local asymptotic stable equilibrium point. Formally, the ROA can be defined as:

$$S = \{x^0 \in R^n \mid \lim_{t \rightarrow \infty} x(t, x^0) = 0\} \quad (6)$$

The estimation of ROA is to explore the system’s specific stable area. It is difficult to compute the ROA exactly for nonlinear dynamical systems, and there has been significant research devoted to the ROA’s invariant subsets estimation.

Figure 2 The fitting effect of  $C_z$

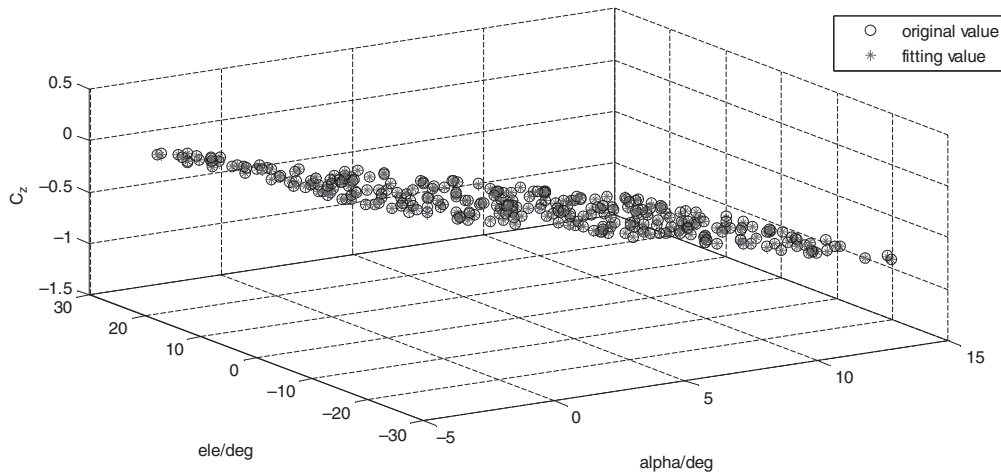
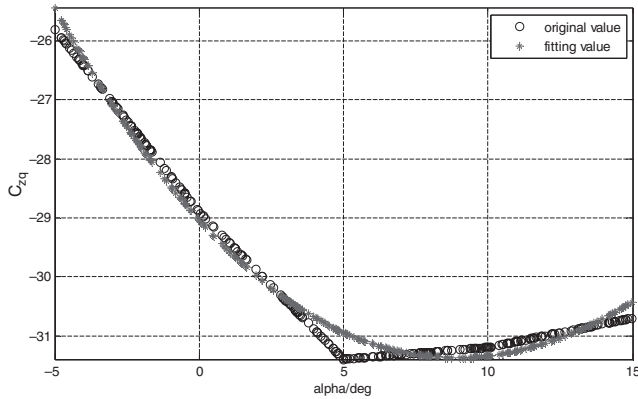


Figure 3 The fitting effect of  $C_{zq}$



Lemma 1 (Tan, 2006; Chakraborty, 2011; Khodadadi, 2014): If there exists a continuous differentiable function  $V: R^n \rightarrow R$  such that:

- $V$  is positive definite;
- $\Omega = \{x \in R^n \mid V(x) \leq 1\}$  is bounded; and
- $\{x \in R^n \mid V(x) \leq 1\} \setminus \{0\} \subseteq \{x \in R^n \mid \frac{\partial V}{\partial x} f(x) < 0\}$ ,

then for all  $x(0) \in \Omega$ , the solution of equation (5) exists, and  $x(t) \in \Omega$ ,  $\lim_{t \rightarrow \infty} x(t) = 0$ . As such, if  $\Omega$  is invariant and a subset of the ROA for equation (5), then the continuous differentiable function  $V$  is called a local Lyapunov function.

Figure 6 shows that the ROA  $\Omega$  defined by the solid line is an elliptical zone,  $\dot{V}(x) = 0$  defined by the dotted-dashed line is the boundary between positive and negative definite zone of  $V(x)$ , system ROA estimation process is finding the maximum ROA in the negative definite area in which  $\dot{V}(x) < 0$ , and the  $\gamma$  is the maximum value.

To enlarge  $\Omega$ , we define a variable-sized region (Jarvis-Wloszek, 2003):

$$P_\beta = \{x \in R^n \mid p(x) \leq \beta\} \quad (7)$$

and then maximize  $\beta$  with the constraint  $P_\beta \subseteq \Omega$ . Here,  $\beta$  is a positive value and  $p(x)$  is a positive definite polynomial, which is

chosen to reflect the different state parameters' relative importance degree, and  $p(x)$  is called the shape factor. With the application of the Lemma 1 above, the problem can be transformed to the following optimization problem (Jarvis-Wloszek, 2003):

$\max \beta$ , subject to:

- $V(x) > 0$  for all  $x \in R^n \setminus \{0\}$  and  $V(0) = 0$ ;
- the set  $\{x \in R^n \mid V(x) \leq 1\}$  is bounded;
- $\{x \in R^n \mid p(x) \leq \beta\} \subseteq \{x \in R^n \mid V(x) \leq 1\}$ ; and
- $\{x \in R^n \mid V(x) \leq 1\} \setminus \{0\} \subseteq \{x \in R^n \mid \frac{\partial V}{\partial x} f < 0\}$ .

Using the S-procedure and SOS programming (Tan, 2006), the following sufficient conditions can be obtained on the basis of optimization conditions above:

$\max \beta$ , subject to:

- $V \in R^n, V(0) = 0, s_1, s_2 \in \sum_n$
- $-[(\beta - p)s_1 + (V - 1)] \in \sum_n$ ; and
- $-[(1 - V)s_2 + \frac{\partial V}{\partial x} f + l_2] \in \sum_n$ .

where  $s_1$  and  $s_2$  are SOS polynomials and  $l_i(x)$  is a positive definite polynomial:

$$l_i = \sum_{j=1}^n \varepsilon_{ij} x_j^2 \quad (8)$$

$i = 1, 2$  and  $\varepsilon_{ij}$  are positive numbers.

### Advanced V-s iteration algorithm for region-of-attraction estimation

The constraint equations above contain some unknown variables, such as  $\beta$  and  $V$ , and their products, such as the product of  $\beta$  and  $s_1$ ,  $V$  and  $s_2$ . In numerical solving process, these products make the SOS problem untranslatable into a linear SDP, which is named as bilinear problem.

To solve this bilinear problem, V-s iteration method will be introduced. The basic idea of V-s iteration method is to divide the unknown variables into two groups. During this process, the two items in product should be divided into different groups, and one decision variable group should be fixed to solve the problem of another group so that the SOS problem can be transformed into linear SDP.



Figure 4 The fitting effect of  $C_m$

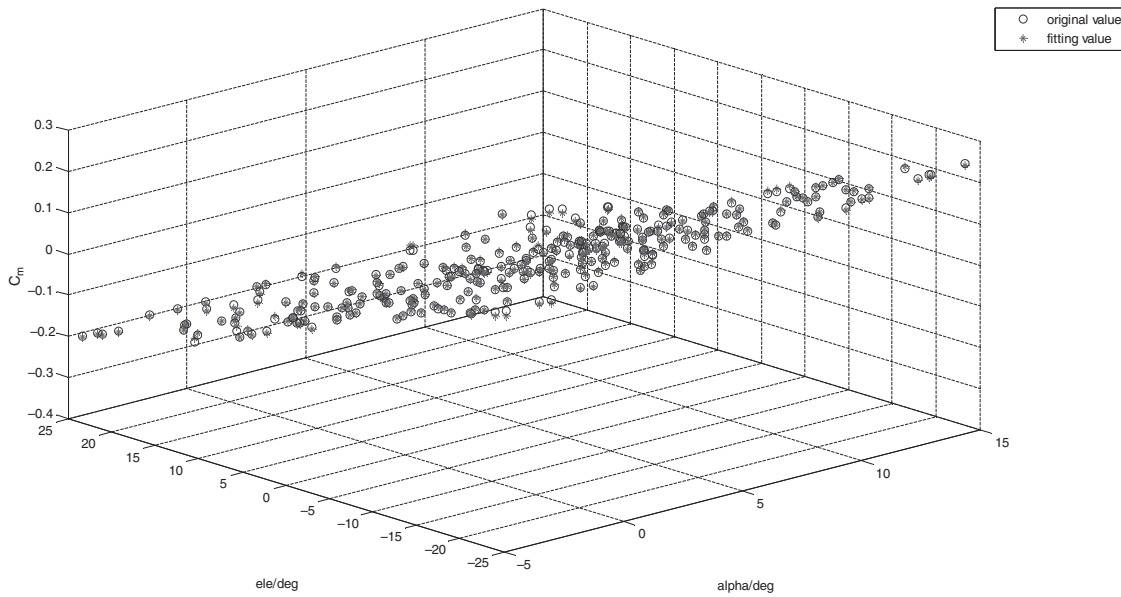
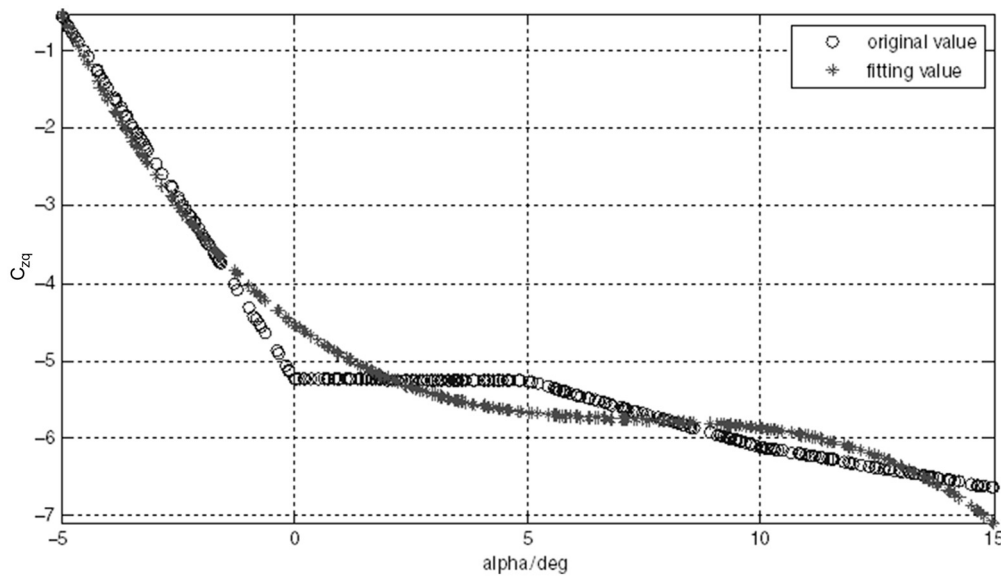


Figure 5 The fitting effect of  $C_{mq}$



Moreover, the optimization problem's constraints conditioned below:

$$\left\{ x \in R^n \mid p(x) \leq \beta \right\} \subseteq \left\{ x \in R^n \mid V(x) \leq 1 \right\},$$

shows that the variable sized region  $P_\beta$  is contained in the system's ROA, or we can say that  $P_\beta$  with different "radius  $\beta$ " is used to enlarge or optimize the ROA. So the relationship between shaper factor  $p(x)$  selection and Lyapunov  $V(x)$  is very

strong, and the selection of  $p(x)$  will affect the ROA's optimization.

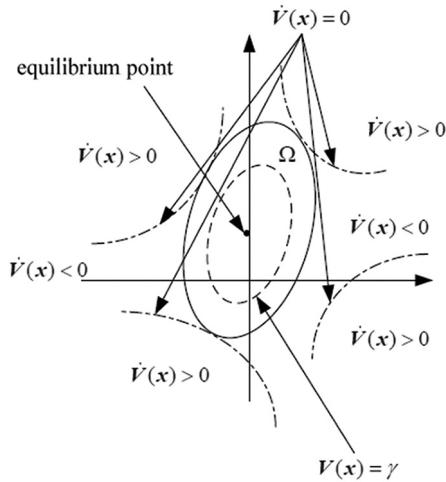
To solve these problems, the advanced V-s iteration algorithm for ROA estimation is (Khodadadi *et al.*, 2014):

- 1 Initialization. Compute the Jacobian matrix of  $f$  evaluated at  $x = 0$ :

$$A = \left. \frac{\partial f(x)}{\partial x} \right|_{x=0} \quad (9)$$

Then solve the equation:

Figure 6 ROA estimation diagram



$$A^T P + PA = -I, \tag{10}$$

to get a positive definite matrix P. Define

$$V(x) = x^T P x \tag{11}$$

$$p(x) = x^T P x \tag{12}$$

2  $\gamma$  Step. Hold  $V$  fixed and solve the following SOS programming for  $s_2(x)$ :

$\max \gamma^*$ , subject to:

$$s_2 \in \sum_n, \gamma \in R$$

$$-\left[ (\gamma - V)s_2 + \frac{\partial V}{\partial x} f + l_2 \right] \in \sum_n,$$

where  $l_2$  is defined in equation (8). The product problem of  $\gamma$  and  $s_2$  can be solved by the conventional V-s iteration approach (Chakraborty et al., 2011).

3  $\beta$  Step. Hold  $V$  and  $p$  fixed and solve the following SOS programming for  $s_1(x)$ :

$\max \beta^*$ , subject to:

$$s_1 \in \sum_n, \beta \in R$$

$$-[(\beta - p)s_1 + (V - \gamma)] \in \sum_n.$$

Similarly, such bilinear problem can be solved by the conventional V-s iteration approach.

4  $V$  Step. Hold  $s_1, s_2, \beta^*, \gamma^*$  and  $p$  fixed and compute  $V$  such that:

$$-\left[ \frac{\partial V}{\partial x} f + l_2 + s_2(\gamma - V) \right] \in \sum_n,$$

$$-[(V - \gamma) + s_1(\beta - p)] \in \sum_n$$

and

$$V - l_1 \in \sum_n, \quad V(0) = 0,$$

where  $l_1$  is defined in the form of equation (8).

- 5 Scale  $V$ . Replace  $V$  with  $V/\gamma^*$ . In this step, a new  $V$  is obtained which satisfies the constraints of the problem.
- 6 Update  $p$ . Replace the quadratic part of the new  $V$  as new  $p$ .
- 7 Repeat. Now with the new  $V$  and new  $p$ , repeat the algorithm to reach to the maximum number of iterations.

To clearly demonstrate the optimization loop process of this advanced V-s iteration algorithm, the algorithm flow chart is drawn as shown in Figure 7.

The maximum times of  $V, s_1$  and  $s_2$  are restricted in this algorithm, that is, the highest order of these polynomials should satisfy:

$$\begin{aligned} \deg V &\geq \deg l_1 \\ \deg(p s_1) &\geq \deg V \\ \deg s_2 &\geq \deg f - 1 \end{aligned} \tag{13}$$

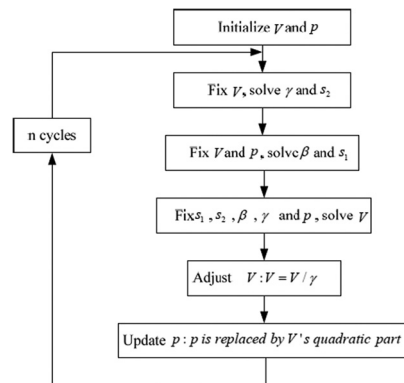
where  $\deg(*)$  defines the highest order of expression.

### The region-of-attraction overlapping estimation

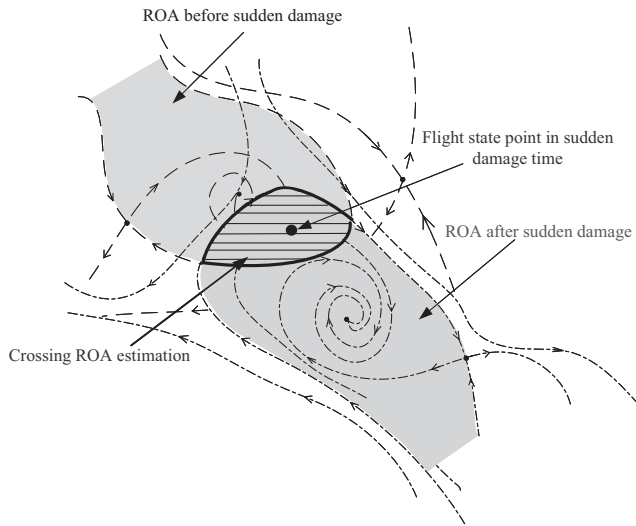
Generally speaking, system ROA determines the safe operation envelopes or stability region of aircraft. Aircraft's sudden damage will change the aerodynamic characteristic or reduce aerodynamic efficiency, and then the aircraft's ROA will be changed as some coefficient's variation in equation (1). If we can analyze and estimate the ROA overlapping between the systems before and after damage as shown in Figure 8, then such ROA overlapping can be used to analyze and evaluate the stability of aircraft's sudden damage process, and moreover, to guarantee flight safety during such sudden damage process.

Figure 8 shows the typical ROA variation of aircraft with sudden damage process. The  $x$ - and  $y$ -axes in the plane indicate two variables of aircraft, and the dotted line and dotted-dashed line define the phase trajectory of the system before and after sudden damage; the current flight state is indicated by the black point in the figure. If these two ROAs have overlapping area shown as the shaded area in Figure 8, and meanwhile, the flight state point at the damage moment is in this overlapping area, it means that this flight state is stable both before and after sudden damage; in other words, the aircraft's sudden damage process is stable.

Figure 7 Advanced V-s iteration algorithm flowchart



**Figure 8** Schematic diagram of ROA overlapping during damage process



Based on the advanced V-s iteration algorithm for ROA estimation above, the ROA  $V_b = \gamma_b$  for the system before damage and ROA  $V_a = \gamma_a$  for the system after damage can be determined, and then the equation set can be used to complete the ROA overlapping estimation:

$$\text{Crossing ROA}(x) = \text{ROA}_{\text{before}}(x) \cap \text{ROA}_{\text{after}}(x)$$

which  $x$  subject to  $V_b(x) \leq \gamma_b$  and  $V_a(x) \leq \gamma_a$

### The stability analysis of aircraft's sudden damage process

For the aircraft before damage and after damage, with the same flight state (i.e. the same flight speed and altitude), the ROAs are estimated in this section. And then through the variation analysis of damage system's ROAs, the stability analysis of aircraft's sudden damage process is completed. And during this procedure, the normal system's ROA is taken as a reference.

#### Region-of-attraction estimation of normal aircraft system

The normal aircraft's polynomial system equations shown in Appendix below is trimmed in level flight, and the initial trim flight condition is  $V = 800 \text{ ft/s}$  and  $H = 20,000 \text{ ft}$ ; the trim results are shown as Table III. To complete the ROA estimation, we

**Table III** Level flight trim results

Flight state parameter	Original model	Polynomial fitting model
$V$ (ft/s)	800	800
$\alpha$ (deg)	1.2818	1.2657
$q$ (rad/s)	0	0
$\theta$ (deg)	1.2818	1.2657
$T$ (lbs)	2,805.2064	3,094.4076
$\delta_e$ (deg)	-1.6982	-1.7938

set the SOS solving equations' parameters in the section above as follows. And the total programming iteration steps are  $N = 100$  (Table IV).

For the  $\gamma$  step and  $\beta$  step in the section mentioned above, the optimization loop overflow condition or tolerance is  $\Delta\gamma = \Delta\beta = 1.0e^{-5}$ , and the initial value is  $\gamma_0 = \beta_0 = 0.01$ . The  $l_i(x)$  is defined as:

$$l_1 = 1.0e^{-6}(\alpha^2 + q^2)$$

and

$$l_2 = 1.0e^{-6}(\alpha^2 + q^2).$$

With the advanced V-s iteration algorithm in the above section, the ROA estimation results can be determined as following:

$$\beta = 1.0096,$$

$$\gamma = 1.0000,$$

$$V(x) = 24.189\alpha^6 - 5.0926\alpha^5q + 18.017\alpha^4q^2 - 49.722\alpha^4 + 8.8848\alpha^3q^3 + 8.9314\alpha^3q + 0.70416\alpha^2q^4 - 3.7347\alpha^2q^2 + 47.192\alpha^2 + 1.4603\alpha q^5 - 15.762\alpha q^3 + 23.608\alpha q + 4.6706q^6 - 5.887q^4 + 11.972q^2$$

and

$$p(x) = 47.218\alpha^2 + 23.585\alpha q + 11.965q^2,$$

then the aircraft's ROA before damage can be plotted as shown in Figure 9.

In Figure 9, the solid line ellipse region  $V(x) < \gamma$  is the normal aircraft's ROA, the dashed-dotted line ellipse region  $p(x) < \beta$  is the shape factor, and the dotted line is the valid range of  $\alpha$ :  $[-5 \text{ to } 15 \text{ deg}]$  (i.e. the valid range of polynomial fitting). So the shadow area is the valid ROA of normal aircraft. And if the flight state is contained in such region, the aircraft system can converge to the initial state point when it confronts external or internal disturbance.

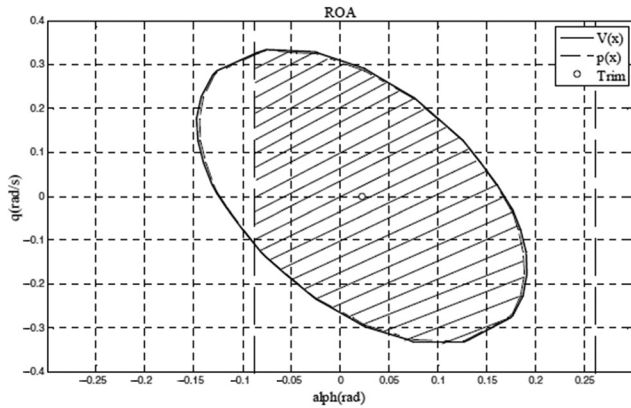
#### Region-of-attraction estimation of damage aircraft system

First of all, the parameters are set as same as in the SOS solving process in the above subsection. With the advanced V-s iteration algorithm in the above section, the ROA estimation results can be determined as following.

**Table IV** SOS programming parameter settings

$f$	6
$V$	6
$p$	2
$s_1$	4
$s_2$	6
Function order	6

Figure 9 ROA of normal system



Damage model

- Thirty per cent damage in tail:

$$\beta = 0.9942, \gamma = 1.0000,$$

$$V(x) = 16.446\alpha^6 - 14.522\alpha^5q + 12.548\alpha^4q^2 - 35.633\alpha^4 + 18.19\alpha^3q^3 + 37.091\alpha^3q + 1.0083\alpha^2q^4 + 39.895\alpha^2q^2 + 49.586\alpha^2 - 2.7325\alpha q^5 - 2.7335\alpha q^3 + 19.86\alpha q + 7.7149q^6 - 9.4061q^4 + 14.882q^2,$$

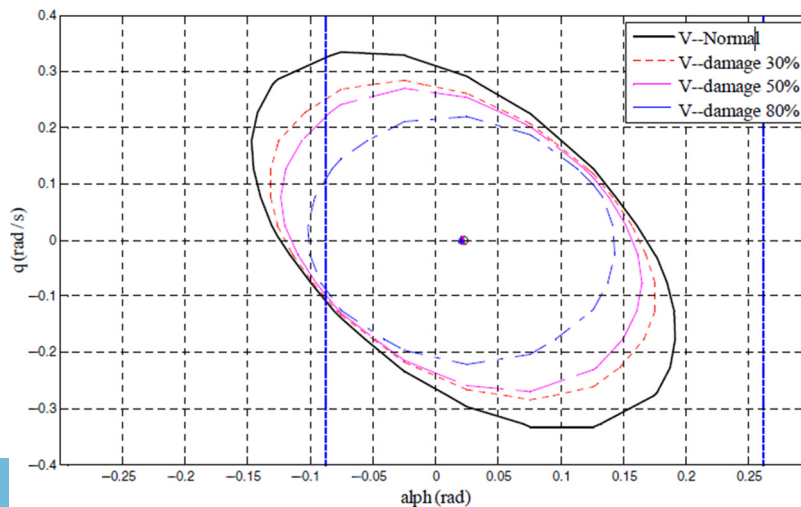
$$p(x) = 49.471\alpha^2 + 19.822\alpha q + 14.931q^2.$$

- Fifty per cent damage in tail:

$$\beta = 0.9968, \gamma = 1.002,$$

$$V(x) = 44.997\alpha^6 - 23.976\alpha^5q - 8.7646\alpha^4q^2 - 72.833\alpha^4 + 24.013\alpha^3q^3 + 23.099\alpha^3q + 12.47\alpha^2q^4 + 67.467\alpha^2q^2 + 53.68\alpha^2 - 0.48176\alpha q^5 - 0.59924\alpha q^3 + 17.658\alpha q + 12.793q^6$$

Figure 10 ROA of damage system



$$- 14.252q^4 + 15.901q^2,$$

$$p(x) = 53.812\alpha^2 + 17.646\alpha q + 15.859q^2.$$

- Eighty per cent damage in tail:

$$\beta = 0.9973, \gamma = 1.0010,$$

$$V(x) = 48.484\alpha^6 - 9.601\alpha^5q - 11.675\alpha^4q^2 - 75.645\alpha^4 + 2.4191\alpha^3q^3 - 6.1565\alpha^3q + 21.456\alpha^2q^4 + 60.516\alpha^2q^2 + 61.884\alpha^2 + 6.846\alpha q^5 + 28.768\alpha q^3 + 9.8624\alpha q + 14.65q^6 - 16.239q^4 + 19.38q^2$$

$$p(x) = 62.015\alpha^2 + 10.033\alpha q + 19.354q^2.$$

Stability analysis and simulation

Based on the optimization results above, the ROA of normal and damage aircraft can be plotted as shown in Figure 10.

Figure 10 shows that, as the aircraft control surface is damaged, the system's ROA will be reduced gradually both along the  $\alpha$  and  $q$  directions, and all the damage systems' ROA are contained in the normal system's ROA, which means that the sudden damage will affect and deteriorate the system's stability, but this effect is not drastic. The bigger deflection angle of control surface within the allowable range should be used to compensate the damage's effect.

Moreover, at the sudden damage moment if the flight state is contained in the overlapping area (intersection of ROAs before and after damage), then the system will be converged to the stable state on the basis of the definition of ROA. On contrary, the system will be divergent and instable.

With the aircraft's tail damage, the aircraft's response curves as the elevator  $\delta_e$ 's disturbance ( $\pm 1$  deg based on the control surface's trimming value) can be simulated and plotted as shown in Figures 11-15.



Figure 11 Airspeed responses with disturbance

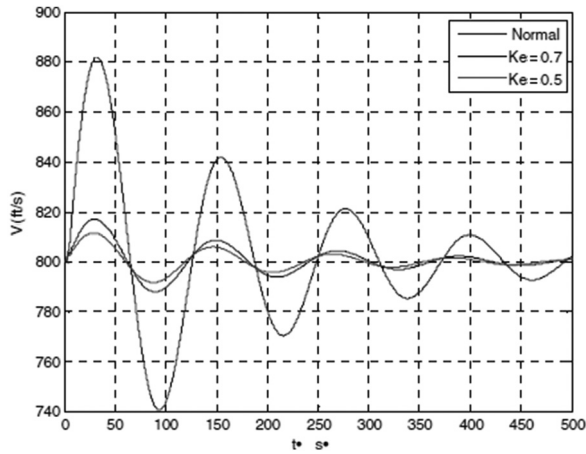


Figure 12 Angle of attack responses with disturbance

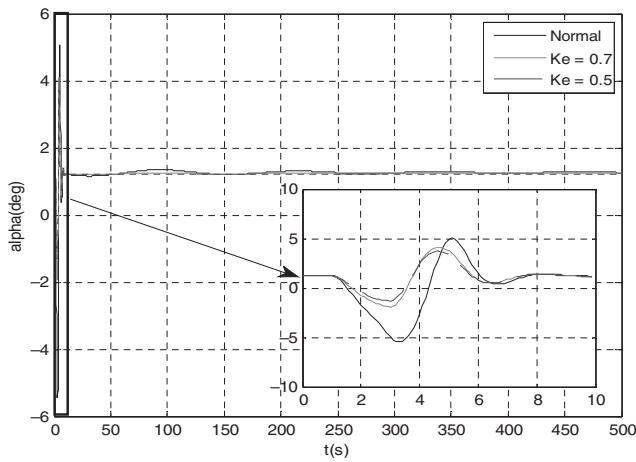


Figure 13 Pitch angle rate responses with disturbance

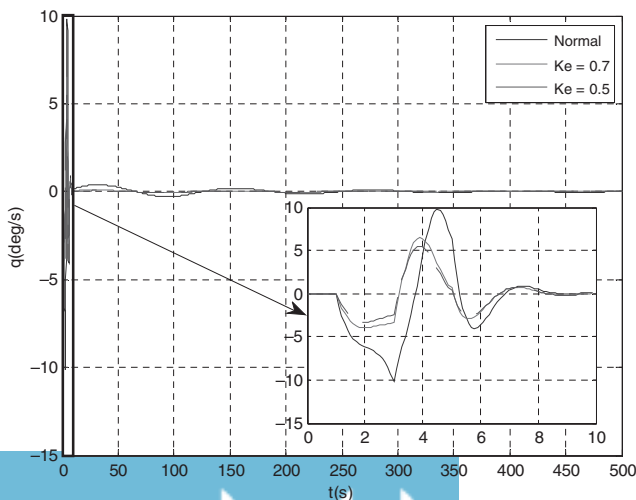


Figure 14 Pitch angle responses with disturbance

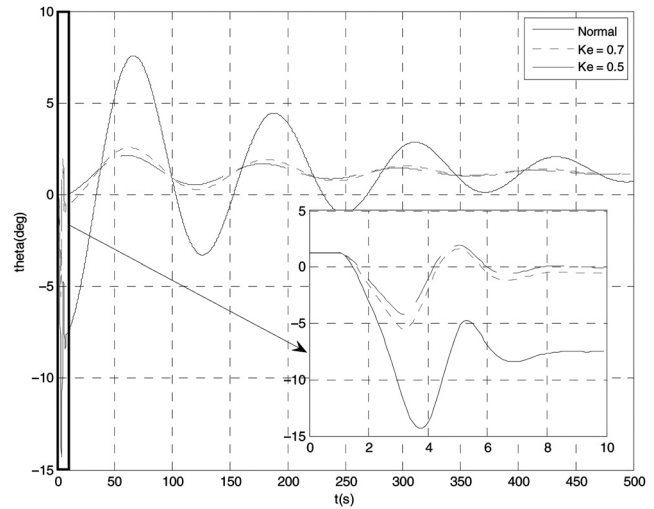
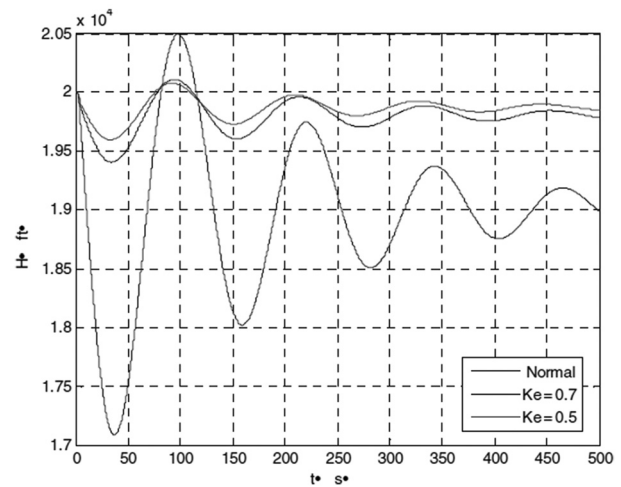


Figure 15 Flight height responses with disturbance



Compared with the normal system, the  $\alpha$ ,  $q$  and  $\theta$ 's trend is the same, but the amplitude is smaller than the normal system which is inversely proportional to the damage degree, and the control efficiency of elevator becomes smaller in the same time.

### Conclusion

The stability analysis method of aircraft's sudden damage is studied with the ROA overlapping in this paper. The main contribution of this paper is to present a new method for evaluating aircraft's stability with sudden damage, which is helpful to consider sudden damage and guarantee flight safety. Through the damage failure analysis and polynomial aerodynamic modelling, the ROA overlapping method can be used to evaluate the aircraft system stability or improve the control law design.

## Further work

Further consideration can focus on emergency controller design which can enlarge the closed-loop system's ROA, and improve flight safety.

## References

- Amato, F., Calabrese, F., Cosentino, C. and Merola, A. (2011), "Stability analysis of nonlinear quadratic systems via polyhedral Lyapunov functions", *Automatica*, Vol. 47 No. 3, pp. 614-617.
- Belcastro, C.M. (2003), "On the validation of safety critical aircraft systems, Part I: An overview of analytical and simulation methods", *AIAA Guidance, Navigation, and Control Conference and Exhibit, Austin, Texas*.
- Brian, L.S. and Frank, L.L. (1992), *Aircraft Control and Simulation*, John Wiley & Sons, NJ.
- Chakraborty, A., Seiler, P. and Balas, G. (2011), "Nonlinear region of attraction analysis for flight control verification and validation", *Control Engineering Practice*, Vol. 19 No. 4, pp. 335-345.
- Chen, X.J. (2009), "Estimation domain of attraction based on bilinear matrix inequalities and sum of squares optimization", PHD Thesis, Northeastern University, ShenYang.
- Cheng, D.Z. (2004), "Stabilization of planar switched systems", *Systems and Control Letters*, Vol. 51 No. 2, pp. 79-88.
- Chesi, G. (2011), *Domain of Attraction: Analysis and Control via SOS Programming*, Springer, London.
- Jackson, E.A. and Kodoeorgiou, A. (1992), "Entrainment and migration controls of two-dimensional maps", *Physic Letter D: Nonlinear Phenomena*, Vol. 54 No. 3, pp. 253-265.
- Jarvis-Wloszek, Z.W. (2003), *Lyapunov Based Analysis and Controller Synthesis for Polynomial Systems Using Sum-of-Squares Optimization*, University of California, Berkeley.
- Jia, H.W., Wang, W., Yu, X.D. and Cao, S.C. (2005), "Tentative study on differential topological characteristics of the small signal stability region part one illustration of nonconvex boundary and instability region (hole) in small signal stability region", *Automation of Electric Power Systems*, Vol. 29 No. 20, pp. 20-23.
- Khodadadi, L., Samadi, B. and Khaloozadeh, H. (2014), "Estimation of region of attraction for polynomial nonlinear systems: a numerical method", *ISA Transactions*, Vol. 53 No. 1, pp. 25-32.
- Papachristodoulou, A. (2005), *Scalable Analysis of Nonlinear Systems Using Convex Optimization*, California Institute of Technology, Pasadena, CA.
- Parrilo, P.A. (2000), *Structured Semi-Definite Programs and Semi-Algebraic Geometry Methods in Robustness and Optimization*, California Institute of Technology, Pasadena, CA.
- Prajna, S. (2005), *Optimization-Based Methods for Nonlinear and Hybrid Systems Verification*, California Institute of Technology, Pasadena, CA.
- Rezgui, D. and Lowenberg, M.H. (2014), "Continuation and bifurcation analysis in helicopter aeroelastic stability problems", *Journal of Guidance, Control, and Dynamics*, Vol. 37 No. 3, pp. 889-897.
- Russell, R.S. (2003), *Non-linear F-16 Simulation using Simulink and Matlab*, University of Minnesota, Version 1.0, 22 June.
- Shorten, R., Narendra, K.S. and Mason, O. (2003), "On common quadratic Lyapunov functions for pairs of stable LTI system whose systems matrices are in companion form", *IEEE Transactions on Automatic Control*, Vol. 48 No. 4, pp. 618-621.
- Tan, W.H. (2006), *Nonlinear Control Analysis and Synthesis Using Sum-of-Squares Programming*, University of California, Berkeley.
- Tu, J.Z., Gan, D.Q., Xin, H.H. and Cao, J. (2012), "Phase portrait analysis of AC/DC power system stability region based on a full state DC model", *Power System Protection and Control*, Vol. 40 No. 21, pp. 58-66.
- Yang, Y.H. (2012), "Study on practical stability domain estimation of a class of nonlinear dynamical system with application", *Mathematics in Practice and Theory*, Vol. 42 No. 13, pp. 189-192.

## Further reading

- Tan, W.H. and Packard, A. (2006), "Stability region analysis using sum of squares programming", *Proceedings of the 2006 American Control Conference in Minneapolis, IEEE, Minnesota*, pp. 2297-2302.

## Corresponding author

Jie Chen can be contacted at: [shuimujie@mail.nwpu.edu.cn](mailto:shuimujie@mail.nwpu.edu.cn)

## Appendix

### Normal longitudinal polynomial system:

$$\begin{aligned} \dot{V} = & 1.5700e^{-3}T + 3.2170e^1\alpha - 3.2170e^1\theta - 7.8500e^{-4}T\alpha^2 - 4.7465e^{-6}V^2\delta_e - 1.4018e^{-7}V^2\delta_e + 4.2831e^{-6}V^2q \\ & - 7.7172e^{-9}V^3q + 4.3885e^{-12}V^4q - 1.6085\delta_e\alpha\theta^2 + 1.6085\delta_e\alpha^2\theta - 7.1181e^{-6}V^2 - 5.3617e^0\alpha^3 + 5.3617e^0\theta^3 \\ & - 8.0905e^{-4}V^2\alpha^2 + 7.9854e^{-4}V^2\alpha^3 - 1.0695e^{-3}V^2\alpha^4 - 2.7266e^{-4}V^2\alpha^5 + 1.8432e^{-4}V^2\alpha^6 \\ & - 9.7300e^{-5}V^2\delta_e^2 + 5.4563e^{-6}V^2\delta_e^3 - 5.9845e^{-5}V^2\alpha\delta_e^2 \\ & - 7.9635e^{-5}V^2\alpha^2\delta_e + 1.4022e^{-6}V^2\alpha\delta_e^3 + 3.7159e^{-5}V^2\alpha^3\delta_e + 3.9976e^{-5}V^2\alpha^4\delta_e \\ & - 1.5017e^{-5}V^2\alpha^2q + 2.0858e^{-4}V^2\alpha^3q + 2.7057e^{-8}V^3\alpha q - 4.0439e^{-4}V^2\alpha^4q - 3.7582e^{-7}V^3\alpha^3q \\ & - 1.5386e^{-11}V^4\alpha^2q + 2.4715e^{-4}V^2\alpha^5q + 7.2862e^{-7}V^3\alpha^4q + 2.1372e^{-10}V^4\alpha^3q + 5.1736e^{-5}V^2\alpha^6q - 4.4531e^{-7}V^3\alpha^5q \\ & - 4.1435e^{-10}V^4\alpha^4q - 9.3216e^{-8}V^3\alpha^6q + 2.5323e^{-10}V^4\alpha^5q + 5.3009e^{-11}V^4\alpha q + 4.8650e^{-5}V^2\alpha^2\delta_e^2 \\ & - 2.7281e^{-6}V^2\alpha^2\delta_e^3 + 2.9898e^{-5}V^2\alpha^3\delta_e^2 - 2.3370e^{-7}V^2\alpha^3\delta_e^3 - 1.6125e^{-4}V^2\alpha\delta_e - 2.1224e^{-4}V^2\alpha q + 3.8242e^{-7}V^3\alpha q \\ & - 2.1747e^{-10}V^4\alpha q; \end{aligned}$$

$$\begin{aligned} \dot{\alpha} = & q - 3.3318e^{-4}V - 9.0247e^{-6}T\alpha + 1.8492e^{-1}\alpha\theta + 1.5041e^{-6}T\alpha^3 + 1.6659e^{-4}V\alpha^2 - 6.3375e^{-6}V^2\alpha + 1.1419e^{-8}V^3\alpha \\ & - 6.4935e^{-12}V^4\alpha - 7.4953e^{-7}V^2\delta_e + 1.3505e^{-9}V^3\delta_e - 7.6798e^{-13}V^4\delta_e - 1.6225e^{-6}V^2q + 5.8467e^{-9}V^3q \\ & - 8.5921e^{-12}V^4q + 5.9906e^{-15}V^5q - 1.7033e^{-18}V^6q + 1.6659e^{-4}V\theta^2 + 1.6981e^{-8}V^2 + 3.1079e^{-10}V^3 - 1.7674e^{-13}V^4 \\ & - 9.2460e^{-2}\alpha^2 - 9.2460e^{-2}\theta^2 + 2.0955e^{-6}V^2\alpha^2 - 4.8822e^{-6}V^2\alpha - 3.9463e^{-9}V^3\alpha^2 \\ & - 3.4852e^{-6}V^2\alpha^4 + 8.7967e^{-9}V^3\alpha^3 + 2.2441e^{-12}V^4\alpha^2 + 3.4632e^{-6}V^2\alpha^5 + 6.2797e^{-9}V^3\alpha^4 \\ & - 5.0024e^{-12}V^4\alpha^3 + 3.9748e^{-7}V^2\alpha^6 - 6.2399e^{-9}V^3\alpha^5 - 3.5710e^{-12}V^4\alpha^4 \\ & - 7.1617e^{-10}V^3\alpha^6 + 3.5484e^{-12}V^4\alpha^5 + 4.0726e^{-13}V^4\alpha^6 - 4.1593e^{-10}V^2\delta_e^2 + 8.0601e^{-9}V^2\delta_e^3 + 7.4941e^{-13}V^3\delta_e^2 \\ & - 1.4523e^{-11}V^3\delta_e^3 - 4.2616e^{-16}V^4\delta_e^2 + 8.2585e^{-15}V^4\delta_e^3 \\ & - 9.4736e^{-8}V^2\theta^2 + 1.5411e^{-12}TV^2\alpha^3 + 5.5930e^{-7}V^2\alpha\delta_e^2 + 5.5212e^{-7}V^2\alpha^2\delta_e - 3.1364e^{-8}V^2\alpha\delta_e^3 + 4.5909e^{-7}V^2\alpha^3\delta_e \\ & - 1.0077e^{-9}V^3\alpha\delta_e^2 - 9.9480e^{-10}V^3\alpha^2\delta_e - 2.9559e^{-8}V^2\alpha^4\delta_e \end{aligned}$$

$$\begin{aligned} & - 3.9463e^{-9}V^3\alpha^2 - 3.4852e^{-6}V^2\alpha^4 + 8.7967e^{-9}V^3\alpha^3 + 2.2441e^{-12}V^4\alpha^2 + 3.4632e^{-6}V^2\alpha^5 + 6.2797e^{-9}V^3\alpha^4 \\ & - 5.0024e^{-12}V^4\alpha^3 + 3.9748e^{-7}V^2\alpha^6 - 6.2399e^{-9}V^3\alpha^5 - 3.5710e^{-12}V^4\alpha^4 \\ & - 7.1617e^{-10}V^3\alpha^6 + 3.5484e^{-12}V^4\alpha^5 + 4.0726e^{-13}V^4\alpha^6 - 4.1593e^{-10}V^2\delta_e^2 + 8.0601e^{-9}V^2\delta_e^3 + 7.4941e^{-13}V^3\delta_e^2 \\ & - 1.4523e^{-11}V^3\delta_e^3 - 4.2616e^{-16}V^4\delta_e^2 + 8.2585e^{-15}V^4\delta_e^3 \\ & - 9.4736e^{-8}V^2\theta^2 + 1.5411e^{-12}TV^2\alpha^3 + 5.5930e^{-7}V^2\alpha\delta_e^2 + 5.5212e^{-7}V^2\alpha^2\delta_e - 3.1364e^{-8}V^2\alpha\delta_e^3 + 4.5909e^{-7}V^2\alpha^3\delta_e \\ & - 1.0077e^{-9}V^3\alpha\delta_e^2 - 9.9480e^{-10}V^3\alpha^2\delta_e - 2.9559e^{-8}V^2\alpha^4\delta_e + 5.6511e^{-11}V^3\alpha\delta_e^3 \\ & - 8.2719e^{-10}V^3\alpha^3\delta_e + 5.7307e^{-13}V^4\alpha\delta_e^2 + 5.6571e^{-13}V^4\alpha^2\delta_e - 7.6716e^{-8}V^2\alpha^5\delta_e + 5.3258e^{-11}V^3\alpha^4\delta_e \\ & - 3.2136e^{-14}V^4\alpha\delta_e^3 + 4.7039e^{-13}V^4\alpha^3\delta_e + 1.3823e^{-10}V^3\alpha^5\delta_e - 3.0286e^{-14}V^4\alpha^4\delta_e - 7.8604e^{-14}V^4\alpha^5\delta_e + 6.3654e^{-6}V^2\alpha^2q \\ & - 2.5720e^{-6}V^2\alpha^3q - 2.2938e^{-8}V^3\alpha^2q + 1.9156e^{-6}V^2\alpha^4q + 9.2684e^{-9}V^3\alpha^3q + 3.3709e^{-11}V^4\alpha^2q + 1.1684e^{-6}V^2\alpha^5q \end{aligned}$$

$$\begin{aligned}
& -6.9030e^{-9}V^3\alpha^4q - 1.3620e^{-11}V^4\alpha^3q - 2.3503e^{-14}V^5\alpha^2q - 8.0448e^{-7}V^2\alpha q \\
& -4.2105e^{-9}V^3\alpha^5q + 1.0144e^{-11}V^4\alpha^4q + 9.4966e^{-15}V^5\alpha^3q + 6.6827e^{-18}V^6\alpha^2q + 2.8990e^{-9}V^3\alpha^6q + 6.1876e^{-12}V^4\alpha^5q \\
& -7.0729e^{-15}V^5\alpha^4q - 2.7002e^{-18}V^6\alpha^3q - 4.2602e^{-12}V^4\alpha^6q \\
& -4.3141e^{-15}V^5\alpha^5q + 2.0111e^{-18}V^6\alpha^4q + 2.9703e^{-15}V^5\alpha^6q + 1.2267e^{-18}V^6\alpha^5q - 8.4457e^{-19}V^6\alpha^6q + 1.6261e^{-8}TV\alpha \\
& -3.3318e^{-4}V\alpha\theta + 3.4379e^{-7}V^2\alpha^2\delta_e^2 - 4.0300e^{-9}V^2\alpha^2\delta_e^3 - 9.3217e^{-8}V^2\alpha^3\delta_e^2 - 6.1944e^{-10}V^3\alpha^2\delta_e^2 + 5.2273e^{-9}V^2\alpha^3\delta_e^3 \\
& -5.7264e^{-8}V^2\alpha^4\delta_e^2 + 7.2613e^{-12}V^3\alpha^2\delta_e^3 + 1.6796e^{-10}V^3\alpha^3\delta_e^2 + 3.5226e^{-13}V^4\alpha^2\delta_e^2 \\
& -9.4184e^{-12}V^3\alpha^3\delta_e^3 + 1.0318e^{-10}V^3\alpha^4\delta_e^2 - 4.1292e^{-15}V^4\alpha^2\delta_e^3 - 9.5511e^{-14}V^4\alpha^3\delta_e^2 + 5.3560e^{-15}V^4\alpha^3\delta_e^3 \\
& -5.8674e^{-14}V^4\alpha^4\delta_e^2 - 9.2469e^{-12}TV^2\alpha - 2.7101e^{-9}TV\alpha^3 + 2.9410e^{-9}V^2\alpha\delta_e - 5.2991e^{-12}V^3\alpha\delta_e + 3.0134e^{-15}V^4\alpha\delta_e \\
& -1.7562e^{-6}V^2\alpha q + 6.3287e^{-9}V^3\alpha q - 9.3004e^{-12}V^4\alpha q + 6.4845e^{-15}V^5\alpha q - 1.8438e^{-18}V^6\alpha q + 1.8947e^{-7}V^2\alpha\theta + 1.8492e^{-1}; \\
\dot{q} = & 1.3605e^{-8}V^3q - 2.2156e^{-5}V^2\delta_e - 7.5507e^{-6}V^2q - 4.6195e^{-6}V^2\alpha - 7.7366e^{-12}V^4q - 5.7692e^{-7}V^2 \\
& -4.8476e^{-5}V^2\alpha^2 + 2.1334e^{-4}V^2\alpha^3 + 1.8541e^{-6}V^2\delta_e^2 + 2.3651e^{-5}V^2\delta_e^3 + 1.4961e^{-5}V^2\alpha\delta_e^2 + 7.7111e^{-6}V^2\alpha^2\delta_e \\
& + 2.4868e^{-4}V^2\alpha^2q - 6.3353e^{-4}V^2\alpha^3q - 4.4807e^{-7}V^3\alpha^2q + 1.1415e^{-6}V^3\alpha^3q + 2.5480e^{-10}V^4\alpha^2q \\
& -6.4913e^{-10}V^4\alpha^3q - 7.7707e^{-6}V^2\alpha\delta_e - 3.4284e^{-5}V^2\alpha q + 6.1772e^{-8}V^3\alpha q - 3.5128e^{-11}V^4\alpha q;
\end{aligned}$$

$$\dot{\theta} = q;$$

### Longitudinal polynomial system with elevator damage 30 per cent:

$$\begin{aligned}
\dot{V} = & 0.00157T + 32.17\alpha - 32.17\theta - 0.000785T\alpha^2 - 4.7041e^{-6}V^2\alpha - 7.504e^{-8}V^2\delta_e + 4.2822e^{-6}V^2q \\
& - 7.7155e^{-9}V^3q + 4.3876e^{-12}V^4q - 16.085\alpha\theta^2 + 16.085\alpha^2\theta - 7.1401e^{-6}V^2 - 5.3617\alpha^3 + 5.3617\theta^3 \\
& - 0.00080655V^2\alpha^2 + 0.00078454V^2\alpha^3 - 0.0010756V^2\alpha^4 - 0.00026593V^2\alpha^5 + 0.00018515V^2\alpha^6 \\
& - 0.000068005V^2\delta_e^2 + 3.604e^{-6}V^2\delta_e^3 - 0.000041506V^2\alpha\delta_e^2 - 0.000055211V^2\alpha^2\delta_e \\
& - 6.5434e^{-7}V^2\alpha\delta_e^3 + 0.000026062V^2\alpha^3\delta_e + 0.000027587V^2\alpha^4\delta_e \\
& - 0.000013933V^2\alpha^2q + 0.00020907V^2\alpha^3q + 2.5104e^{-8}V^3\alpha^2q - 0.00041974V^2\alpha^4q - 3.7669e^{-7}V^3\alpha^3q \\
& - 1.4276e^{-11}V^4\alpha^2q + 0.00024899V^2\alpha^5q + 7.5629e^{-7}V^3\alpha^4q + 2.1421e^{-10}V^4\alpha^3q + 0.000054166V^2\alpha^6q - 4.4862e^{-7}V^3\alpha^5q \\
& - 4.3008e^{-10}V^4\alpha^4q - 9.7595e^{-8}V^3\alpha^6q + 2.5512e^{-10}V^4\alpha^5q + 5.5499e^{-11}V^4\alpha^6q + 0.000034003V^2\alpha^2\delta_e^2 \\
& - 1.802e^{-6}V^2\alpha^2\delta_e^3 + 0.000020735V^2\alpha^3\delta_e^2 + 1.0906e^{-7}V^2\alpha^3\delta_e^3 - 0.00011278V^2\alpha\delta_e \\
& - 0.00021231V^2\alpha q + 3.8254e^{-7}V^3\alpha q - 2.1754e^{-10}V^4\alpha q; \\
\dot{\alpha} = & q - 0.00033318V - 9.0247e^{-6}T\alpha + 0.18492\alpha\theta + 1.5041e^{-6}T\alpha^3 + 0.00016659V\alpha^2 - 6.3357e^{-6}V^2\alpha + 1.1416e^{-8}V^3\alpha \\
& - 6.4917e^{-12}V^4\alpha - 5.2302e^{-7}V^2\delta_e + 9.4236e^{-10}V^3\delta_e - 5.3589e^{-13}V^4\delta_e - 1.6226e^{-6}V^2q \\
& + 5.8471e^{-9}V^3q - 8.5926e^{-12}V^4q + 5.991e^{-15}V^5q - 1.7035e^{-18}V^6q + 0.00016659V\theta^2 + 1.7132e^{-8}V^2 \\
& + 3.1052e^{-10}V^3 - 1.7658e^{-13}V^4 - 0.09246\alpha^2 - 0.09246\theta^2 + 2.0907e^{-6}V^2\alpha^2 - 4.924e^{-6}V^2\alpha^3 - 3.9377e^{-9}V^3\alpha^2
\end{aligned}$$

$$\begin{aligned}
& -3.4071e^{-6}V^2\alpha^4 + 8.8721e^{-9}V^3\alpha^3 + 2.2392e^{-12}V^4\alpha^2 + 3.4794e^{-6}V^2\alpha^5 + 6.1389e^{-9}V^3\alpha^4 - 5.0453e^{-12}V^4\alpha^3 \\
& + 3.8485e^{-7}V^2\alpha^6 - 6.2692e^{-9}V^3\alpha^5 - 3.491e^{-12}V^4\alpha^4 - 6.9341e^{-10}V^3\alpha^6 + 3.5651e^{-12}V^4\alpha^5 + 3.9432e^{-13}V^4\alpha^6 \\
& -3.0436e^{-10}V^2\delta_e^2 - 3.7613e^{-9}V^2\delta_e^3 + 5.4839e^{-13}V^3\delta_e^2 + 6.777e^{-12}V^3\delta_e^3 - 3.1185e^{-16}V^4\delta_e^2 - 3.8539e^{-15}V^4\delta_e^3 \\
& -9.4736e^{-8}V^2\theta^2 + 1.5411e^{-12}TV^2\alpha^3 + 3.9091e^{-7}V^2\alpha\delta_e^2 + 3.8679e^{-7}V^2\alpha^2\delta_e - 2.0717e^{-8}V^2\alpha\delta_e^3 + 3.1719e^{-7}V^2\alpha^3\delta_e \\
& -7.0433e^{-10}V^3\alpha\delta_e^2 - 6.9691e^{-10}V^3\alpha^2\delta_e - 2.088e^{-8}V^2\alpha^4\delta_e + 3.7327e^{-11}V^3\alpha\delta_e^3 - 5.715e^{-10}V^3\alpha^3\delta_e \\
& + 4.0053e^{-13}V^4\alpha\delta_e^2 + 3.9631e^{-13}V^4\alpha^2\delta_e - 5.2822e^{-8}V^2\alpha^5\delta_e + 3.7621e^{-11}V^3\alpha^4\delta_e - 2.1227e^{-14}V^4\alpha\delta_e^3 \\
& + 3.2499e^{-13}V^4\alpha^3\delta_e + 9.5174e^{-11}V^3\alpha^5\delta_e - 2.1394e^{-14}V^4\alpha^4\delta_e - 5.4123e^{-14}V^4\alpha^5\delta_e \\
& + 6.4014e^{-6}V^2\alpha^2q - 2.664e^{-6}V^2\alpha^3q - 2.3068e^{-8}V^3\alpha^2q + 1.9308e^{-6}V^2\alpha^4q + 9.6001e^{-9}V^3\alpha^3q \\
& + 3.39e^{-11}V^4\alpha^2q + 1.212e^{-6}V^2\alpha^5q \\
& -6.9576e^{-9}V^3\alpha^4q - 1.4108e^{-11}V^4\alpha^3q - 2.3636e^{-14}V^5\alpha^2q - 8.0998e^{-7}V^2\alpha^6q \\
& - 4.3677e^{-9}V^3\alpha^5q + 1.0225e^{-11}V^4\alpha^4q + 9.8364e^{-15}V^5\alpha^3q + 6.7205e^{-18}V^6\alpha^2q + 2.9188e^{-9}V^3\alpha^6q + 6.4185e^{-12}V^4\alpha^5q \\
& - 7.1289e^{-15}V^5\alpha^4q - 2.7968e^{-18}V^6\alpha^3q - 4.2894e^{-12}V^4\alpha^6q \\
& - 4.4752e^{-15}V^5\alpha^5q + 2.027e^{-18}V^6\alpha^4q + 2.9907e^{-15}V^5\alpha^6q + 1.2724e^{-18}V^6\alpha^5q - 8.5035e^{-19}V^6\alpha^6q + 1.6261e^{-8}TV\alpha \\
& - 0.00033318V\alpha\theta + 2.3843e^{-7}V^2\alpha^2\delta_e^2 + 1.8806e^{-9}V^2\alpha^2\delta_e^3 - 6.5151e^{-8}V^2\alpha^3\delta_e^2 - 4.296e^{-10}V^3\alpha^2\delta_e^2 + 3.4528e^{-9}V^2\alpha^3\delta_e^3 \\
& - 3.9713e^{-8}V^2\alpha^4\delta_e^2 - 3.3885e^{-12}V^3\alpha^2\delta_e^3 + 1.1739e^{-10}V^3\alpha^3\delta_e^2 + 2.443e^{-13}V^4\alpha^2\delta_e^2 \\
& - 6.2212e^{-12}V^3\alpha^3\delta_e^3 + 7.1555e^{-11}V^3\alpha^4\delta_e^2 + 1.9269e^{-15}V^4\alpha^2\delta_e^3 - 6.6755e^{-14}V^4\alpha^3\delta_e^2 + 3.5378e^{-15}V^4\alpha^3\delta_e^3 \\
& - 4.0691e^{-14}V^4\alpha^4\delta_e^2 - 9.2469e^{-12}TV^2\alpha - 2.7101e^{-9}TV\alpha^3 - 2.1687e^{-10}V^2\alpha\delta_e + 3.9076e^{-13}V^3\alpha\delta_e - 2.2221e^{-16}V^4\alpha\delta_e \\
& - 1.7602e^{-6}V^2\alpha q + 6.343e^{-9}V^3\alpha q - 9.3214e^{-12}V^4\alpha q + 6.4992e^{-15}V^5\alpha q - 1.8479e^{-18}V^6\alpha q + 1.8947e^{-7}V^2\alpha\theta + 0.18492; \\
\dot{q} = & 1.0511e^{-8}V^3q - 0.000015514V^2\delta_e - 5.8335e^{-6}V^2q - 4.5745e^{-6}V^2\alpha - 5.9771e^{-12}V^4q - 4.6354e^{-7}V^2 \\
& - 0.000048945V^2\alpha^2 + 0.00021457V^2\alpha^3 + 1.2997e^{-6}V^2\delta_e^2 + 0.000016627V^2\delta_e^3 + 0.000010535V^2\alpha\delta_e^2 + 6.32e^{-6}V^2\alpha^2\delta_e \\
& e + 0.00017718V^2\alpha^2q - 0.00044739V^2\alpha^3q - 3.1923e^{-7}V^3\alpha^2q + 8.061e^{-7}V^3\alpha^3q + 1.8154e^{-10}V^4\alpha^2q - 4.584e^{-10}V^4\alpha^3q \\
& - 5.5854e^{-6}V^2\alpha\delta_e - 0.000024631V^2\alpha q + 4.438e^{-8}V^3\alpha q - 2.5238e^{-11}V^4\alpha q;
\end{aligned}$$

$$\dot{\theta} = q;$$

### Longitudinal polynomial system with elevator damage 50 per cent:

$$\begin{aligned}
\dot{V} = & 0.00157T + 32.17\alpha - 32.17\theta - 0.000785T\alpha^2 - 4.5062e^{-6}V^2\alpha - 9.6609e^{-8}V^2\delta_e + 4.3059e^{-6}V^2q \\
& - 7.7583e^{-9}V^3q + 4.4119e^{-12}V^4q - 16.085\alpha\theta^2 + 16.085\alpha^2\theta - 7.1236e^{-6}V^2 - 5.3617\alpha^3 + 5.3617\theta^3 \\
& - 0.00081014V^2\alpha^2 + 0.0007935V^2\alpha^3 - 0.0010599V^2\alpha^4 - 0.00027173V^2\alpha^5 + 0.00018284V^2\alpha^6 \\
& - 0.000048609V^2\delta_e^2 + 3.0145e^{-6}V^2\delta_e^3 - 0.000030288V^2\alpha\delta_e^2 - 0.00003733V^2\alpha^2\delta_e \\
& - 6.2497e^{-7}V^2\alpha\delta_e^3 + 0.00001868V^2\alpha^3\delta_e + 0.000018719V^2\alpha\delta_e \\
& - 0.000019337V^2\alpha^2q + 0.000234V^2\alpha^3q + 3.4842e^{-8}V^3\alpha^2q - 0.00044659V^2\alpha^4q - 4.2162e^{-7}V^3\alpha^3q
\end{aligned}$$



$$\begin{aligned}
& -1.9814e^{-11} V^4 \alpha^2 q + 0.00023996 V^2 \alpha^5 q + 8.0467e^{-7} V^3 \alpha^4 q + 2.3976e^{-10} V^4 \alpha^3 q + 0.000059051 V^2 \alpha^6 q \\
& -4.3236e^{-7} V^3 \alpha^5 q - 4.5759e^{-10} V^4 \alpha^4 q - 1.064e^{-7} V^3 \alpha^6 q + 2.4587e^{-10} V^4 \alpha^5 q + 6.0504e^{-11} V^4 \alpha^6 q + 0.000024305 V^2 \alpha^2 \delta_e^2 \\
& -1.5073e^{-6} V^2 \alpha^2 \delta_e^3 + 0.000015139 V^2 \alpha^3 \delta_e^2 + 1.0416e^{-7} V^2 \alpha^3 \delta_e^3 - 0.000080705 V^2 \alpha \delta_e - 0.00021216 V^2 \alpha q \\
& + 3.8226e^{-7} V^3 \alpha q - 2.1738e^{-10} V^4 \alpha q;
\end{aligned}$$

$$\begin{aligned}
\dot{\alpha} = & q - 0.00033318 V - 9.0247e^{-6} T \alpha + 0.18492 \alpha \theta + 1.5041e^{-6} T \alpha^3 + 0.00016659 V \alpha^2 - 6.3345e^{-6} V^2 \alpha + 1.1413e^{-8} V^3 \alpha \\
& - 6.4904e^{-12} V^4 \alpha - 3.7374e^{-7} V^2 \delta_e + 6.7339e^{-10} V^3 \delta_e - 3.8294e^{-13} V^4 \delta_e - 1.6227e^{-6} V^2 q + 5.8474e^{-9} V^3 q \\
& - 8.5932e^{-12} V^4 q + 5.9914e^{-15} V^5 q - 1.7036e^{-18} V^6 q + 0.00016659 V \theta^2 + 1.7093e^{-8} V^2 + 3.1059e^{-10} V^3 - 1.7662e^{-13} V^4 \\
& - 0.09246 \alpha^2 - 0.09246 \theta^2 + 2.0676e^{-6} V^2 \alpha^2 - 4.8231e^{-6} V^2 \alpha^3 - 3.8961e^{-9} V^3 \alpha^2 \\
& - 3.47e^{-6} V^2 \alpha^4 + 8.6901e^{-9} V^3 \alpha^3 + 2.2156e^{-12} V^4 \alpha^2 + 3.4359e^{-6} V^2 \alpha^5 + 6.2521e^{-9} V^3 \alpha^4 \\
& - 4.9418e^{-12} V^4 \alpha^3 + 3.9718e^{-7} V^2 \alpha^6 - 6.1908e^{-9} V^3 \alpha^5 - 3.5554e^{-12} V^4 \alpha^4 \\
& - 7.1562e^{-10} V^3 \alpha^6 + 3.5205e^{-12} V^4 \alpha^5 + 4.0695e^{-13} V^4 \alpha^6 - 9.4302e^{-11} V^2 \delta_e^2 \\
& - 3.5925e^{-9} V^2 \delta_e^3 + 1.6991e^{-13} V^3 \delta_e^2 + 6.4728e^{-12} V^3 \delta_e^3 - 9.6624e^{-17} V^4 \delta_e^2 - 3.6809e^{-15} V^4 \delta_e^3 \\
& - 9.4736e^{-8} V^2 \theta^2 + 1.5411e^{-12} T V^2 \alpha^3 + 2.7942e^{-7} V^2 \alpha \delta_e^2 + 2.7704e^{-7} V^2 \alpha^2 \delta_e - 1.7328e^{-8} V^2 \alpha \delta_e^3 + 2.1502e^{-7} V^2 \alpha^3 \delta_e \\
& - 5.0345e^{-10} V^3 \alpha \delta_e^2 - 4.9917e^{-10} V^3 \alpha^2 \delta_e - 1.5029e^{-8} V^2 \alpha^4 \delta_e + 3.1222e^{-11} V^3 \alpha \delta_e^3 \\
& - 3.8742e^{-10} V^3 \alpha^3 \delta_e + 2.8629e^{-13} V^4 \alpha \delta_e^2 + 2.8386e^{-13} V^4 \alpha^2 \delta_e - 3.5894e^{-8} V^2 \alpha^5 \delta_e + 2.7078e^{-11} V^3 \alpha^4 \delta_e \\
& - 1.7755e^{-14} V^4 \alpha \delta_e^3 + 2.2031e^{-13} V^4 \alpha^3 \delta_e + 6.4674e^{-11} V^3 \alpha^5 \delta_e - 1.5399e^{-14} V^4 \alpha^4 \delta_e \\
& - 3.6778e^{-14} V^4 \alpha^5 \delta_e + 6.4606e^{-6} V^2 \alpha^2 q - 2.8035e^{-6} V^2 \alpha^3 q \\
& - 2.3281e^{-8} V^3 \alpha^2 q + 1.8172e^{-6} V^2 \alpha^4 q + 1.0103e^{-8} V^3 \alpha^3 q + 3.4213e^{-11} V^4 \alpha^2 q + 1.2918e^{-6} V^2 \alpha^5 q - 6.5483e^{-9} V^3 \alpha^4 q \\
& - 1.4847e^{-11} V^4 \alpha^3 q - 2.3854e^{-14} V^5 \alpha^2 q - 7.9603e^{-7} V^2 \alpha^6 q \\
& - 4.655e^{-9} V^3 \alpha^5 q + 9.6231e^{-12} V^4 \alpha^4 q + 1.0351e^{-14} V^5 \alpha^3 q + 6.7826e^{-18} V^6 \alpha^2 q + 2.8686e^{-9} V^3 \alpha^6 q + 6.8409e^{-12} V^4 \alpha^5 q \\
& - 6.7095e^{-15} V^5 \alpha^4 q - 2.9433e^{-18} V^6 \alpha^3 q - 4.2155e^{-12} V^4 \alpha^6 q \\
& - 4.7696e^{-15} V^5 \alpha^5 q + 1.9077e^{-18} V^6 \alpha^4 q + 2.9392e^{-15} V^5 \alpha^6 q + 1.3562e^{-18} V^6 \alpha^5 q - 8.3571e^{-19} V^6 \alpha^6 q + 1.6261e^{-8} T V \alpha \\
& - 0.00033318 V \alpha \theta + 1.7406e^{-7} V^2 \alpha^2 \delta_e^2 + 1.7962e^{-9} V^2 \alpha^2 \delta_e^3 - 4.6569e^{-8} V^2 \alpha^3 \delta_e^2 \\
& - 3.1361e^{-10} V^3 \alpha^2 \delta_e^2 + 2.888e^{-9} V^2 \alpha^3 \delta_e^3 - 2.9001e^{-8} V^2 \alpha^4 \delta_e^2 \\
& - 3.2364e^{-12} V^3 \alpha^2 \delta_e^3 + 8.3908e^{-11} V^3 \alpha^3 \delta_e^2 + 1.7834e^{-13} V^4 \alpha^2 \delta_e^2 \\
& - 5.2036e^{-12} V^3 \alpha^3 \delta_e^3 + 5.2254e^{-11} V^3 \alpha^4 \delta_e^2 + 1.8405e^{-15} V^4 \alpha^2 \delta_e^3 - 4.7716e^{-14} V^4 \alpha^3 \delta_e^2 + 2.9591e^{-15} V^4 \alpha^3 \delta_e^3 \\
& - 2.9715e^{-14} V^4 \alpha^4 \delta_e^2 - 9.2469e^{-12} T V^2 \alpha - 2.7101e^{-9} T V \alpha^3 + 1.0665e^{-9} V^2 \alpha \delta_e - 1.9216e^{-12} V^3 \alpha \delta_e + 1.0928e^{-15} V^4 \alpha \delta_e \\
& - 1.7644e^{-6} V^2 \alpha q + 6.3582e^{-9} V^3 \alpha q
\end{aligned}$$

$$-9.3438e^{-12} V^4 \alpha q + 6.5147e^{-15} V^5 \alpha q - 1.8524e^{-18} V^6 \alpha q + 1.8947e^{-7} V^2 \alpha \theta + 0.18492;$$

$$\begin{aligned}
\dot{q} = & 8.4324e^{-9} V^3 q - 0.000011092 V^2 \delta_e - 4.68e^{-6} V^2 q - 4.5187e^{-6} V^2 \alpha - 4.7952e^{-12} V^4 q - 3.8579e^{-7} V^2 \\
& - 0.000049027 V^2 \alpha^2 + 0.00021344 V^2 \alpha^3 + 9.014e^{-7} V^2 \delta_e^2 + 0.000012003 V^2 \delta_e^3 + 7.5717e^{-6} V^2 \alpha \delta_e^2 + 4.2572e^{-6} V^2 \alpha \delta_e \\
& + 0.00012715 V^2 \alpha^2 q - 0.00031595 V^2 \alpha^3 q - 2.291e^{-7} V^3 \alpha^2 q + 5.6927e^{-7} V^3 \alpha^3 q + 1.3028e^{-10} V^4 \alpha^2 q - 3.2372e^{-10} V^4 \alpha^3 q \\
& - 3.9148e^{-6} V^2 \alpha \delta_e - 0.000018112 V^2 \alpha q + 3.2633e^{-8} V^3 \alpha q - 1.8557e^{-11} V^4 \alpha q;
\end{aligned}$$

$$\dot{\theta} = q;$$

For instructions on how to order reprints of this article, please visit our website:

[www.emeraldgroupublishing.com/licensing/reprints.htm](http://www.emeraldgroupublishing.com/licensing/reprints.htm)

Or contact us for further details: [permissions@emeraldinsight.com](mailto:permissions@emeraldinsight.com)

Reproduced with permission of copyright owner. Further reproduction prohibited without permission.